Electrostrictive generation of nonresonant gratings in the gas phase by multimode lasers

A. Stampanoni-Panariello, B. Hemmerling, and W. Hubschmid
Paul Scherrer Institut, CH-5232 Villigen PSI, Switzerland
(Received 18 March 1994; revised manuscript received 25 August 1994)

Nonresonant gratings have been generated in gases using as excitation beams the second-harmonic output of a multimode Nd:YAG (yttrium aluminum garnet) laser (pulse duration $\tau=8$ ns, coherence time $\tau_c=20$ ps). The grating reflectivity is measured by scattering a probe beam off the grating. It shows the damped oscillation of a standing acoustic wave (period T_p). By varying the time delay τ_d between the excitation beams, the influence of the temporal laser coherence is analyzed. The signal for incoherent excitation ($\tau_c \ll |\tau_d| \ll \tau$) is nonvanishing and depends only weakly on τ_d. It is reduced by about a factor τ_c/τ compared to coherent excitation, if $T_p \gg \tau$. The measurements are interpreted within a calculation of electrostrictively generated gratings from beams having Gaussian temporal pulse shape, Gaussian statistics for the intensity, and a Gaussian frequency spectrum. Furthermore, the measurement of acoustic quantities (sound velocity and attenuation) with the described setup is discussed.

PACS number(s): 42.65.Es, 43.35.+d, 42.25.Kb

I. INTRODUCTION

Two beams originating from a laser and intersecting at an angle θ form an interference pattern which, by various resonant or nonresonant mechanisms, may result in the formation of a dynamic grating. It is described by a periodic complex refractive index [1–3]. Resonantly excited laser-induced gratings are generated by tuning the laser to absorption lines of the medium under investigation. This technique, called laser-induced grating spectroscopy, has found many applications; see, e.g., Refs. [4–8]. Acoustic gratings caused by electrostriction [9], on the other hand, are formed at any frequency of the excitation laser. Here sound waves are generated by the electrostrictive force of the fields in any point of the overlap volume of the laser beams. The wavelength and the direction of the sound waves match the interference geometry. The resulting density change in the beam overlap volume, giving rise to a refractive index change, results from the superposition of the waves coming from opposite directions. They form a spatially periodic density grating which oscillates in time. Electrostrictive gratings have been applied to study acoustic modes and their attenuation and couplings in condensed matter [9,10]. Govoni *et al.* [11] emphasized that electrostrictive gratings should be considered as a nonresonant background in laser-induced grating spectroscopy.

Recently, interest arose in the electrostrictive grating formation in gases [11,12]. In this work, the formation of electrostrictive gratings in gases for partially coherent excitation beams is investigated theoretically and experimentally. Additionally, examples of measurements of acoustic quantities in gases are given (Sec. IV). A variable optical delay line for one of the excitation beams, introducing a time delay τ_d, controls the partial coherence in the experiment. The grating reflectivity is measured by Bragg scattering a probe beam of a second pulsed laser which can be stepwise time delayed with respect to the excitation beams. In the case of coherent excitation beams ($\tau_d=0$), the reflectivity of an electrostrictive grating is given by the integrated intensity of the excitation pulses, if the period T_p of the grating oscillation exceeds definitely the pulse duration τ. For gases, a T_p of many nanoseconds can easily be obtained. In argon, e.g., at an intersection angle θ of 2.9°, T_p is about 16 ns. Therefore, in contrast to experiments in condensed matter with much higher sound velocities, the use of lasers with nanosecond pulse duration is advantageous and results in a stronger grating reflectivity. The mainly acoustic nature of the gratings generated in the experiments is confirmed by the time dependence of their reflectivity, which is in a good approximation a damped oscillation.

In the case of temporally incoherent excitation beams (Sec. V), the coherence time τ_c restricts the integration time of the intensity. For multimode lasers with a small τ_c, this results in a much smaller but still observable grating reflectivity. The stepwise delayed probe beam reveals still the damped oscillation of a standing acoustic wave. For small angles θ, corresponding to $T_p \gg \tau$, it was found that the ratio of the grating reflectivity from temporally coherent and incoherent beams equals about τ/τ_c, in agreement with the calculation of electrostrictive gratings in Sec. III. The application of temporally incoherent excitation beams could be useful in laser-induced grating spectroscopy as it is a method to reduce the nonresonant background, which is one of the limiting factors of the sensitivity. The grating reflectivity as a function of the time delay τ_d, observed with an undelayed probe beam, results in an approximately Gaussian temporal coherence function for the used laser. For $|\tau_d| \gg \tau_c$, an approximately constant and nonvanishing contribution remains.

II. EXPERIMENT

The experimental configuration used to obtain and study electrostrictive gratings in gases is schematically shown in Fig. 1. Two frequency-doubled multimode Nd:YAG (yttrium aluminum garnet) lasers (Continuum

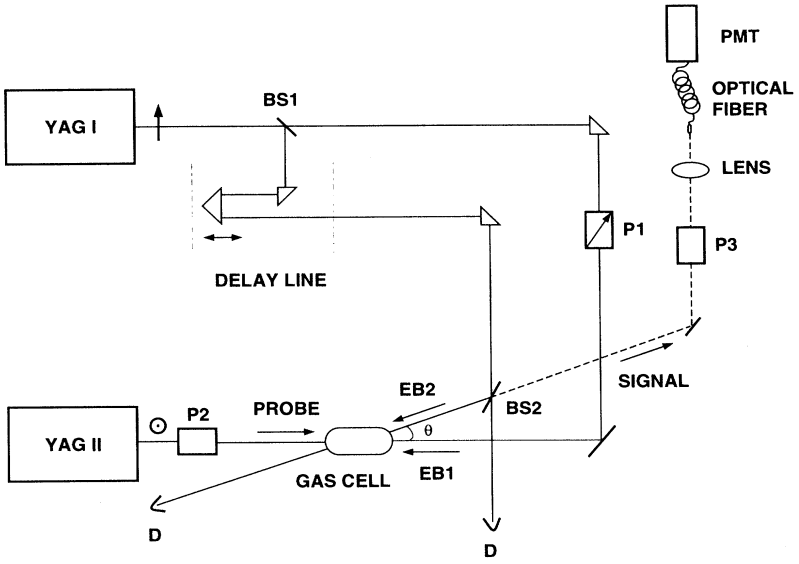

FIG. 1. Experimental setup. BS1 and BS2, beam splitters ($R=50\%$); EB1 and EB2, excitation beams; D, beam dump; P1, P2, and P3, polarizers; PMT, photomultiplier tube.

NY81-20) with a pulse duration of about 8 ns [full width at half maximum (FWHM)] and a beam diameter of about 6 mm are used. The coherence length is measured to be 6 mm; see Sec. V. The output of laser 1 is split by a 50% beam splitter (BS1) into two excitation beams EB1 and EB2, which set up the grating. In order to achieve equal path lengths for these two beams, EB2 passes a delay line formed by two prisms before it is directed by a second 50% beam splitter (BS2) into a gas cell where it crosses EB1 at an angle θ. The gas cell has a variable length and can be used up to a pressure of 5 bar. The output of laser 2 provides the probe beam which is diffracted off the grating into the signal beam. The probe beam is perpendicularly polarized to the excitation beams and is carefully aligned to be counterpropagating to EB1. Hence the polarizers P1 and P2, which are crossed to each other, can be used to protect the lasers against damage from back traveling light. Satisfying the Bragg condition, the signal beam is counterpropagating to EB2. In previous work we found that the signal beam is also phase conjugated to the excitation beam EB2 [12]. Part of the signal beam passes through the beam splitter BS2. Stray light, mainly caused by beam splitter BS2, is efficiently suppressed by polarizer P3 in the path of the signal beam. Furthermore, spatial filtering is achieved by coupling the signal beam into a 200-μm-diam optical fiber (15 m long), which is connected to a photomultiplier tube. The two lasers were electronically synchronized. The time delay between excitation beams and probe beam could be varied by means of a digital delay generator (Stanford Research Systems DG535). The variation of the delay time and the data acquisition was under control of a personal computer.

III. ELECTROSTRICTIVE DENSITY GRATINGS FROM STOCHASTIC FIELDS

We define $\rho'(t,\mathbf{r})$ to be the change in density generated in the medium by the electrostrictive force of the laser excitation beams. The scattering reflectivity of a density grating is proportional to $|\rho'(t,\mathbf{r})|^2$. In addition, the reflectivity depends on the size and the shape of the grating [13]. This latter dependence is outside the scope of this work. Experimentally, for the setup described in Sec. II and an excitation intensity of 90 MW/cm^2 (EB1 and EB2), reflectivities of the order of 10^{-9} are obtained in air at 1 bar.

The linearized equations of fluid dynamics are applied to calculate $|\rho'(t,\mathbf{r})|^2$. Local equilibrium is given as the grating spacing is large compared to the mean free path at the chosen gas pressures and the mean time between two collisions of a molecule is small compared to the pulse duration of the laser and the attenuation constant of the density wave. We consider the equation for $\rho'(t,\mathbf{r})$, which results for a viscous medium when heat transfer is neglected [14]; later, in the discussion of the attenuation of the sound wave (Sec. IV), heat transfer is included phenomenologically:

$$\frac{\partial^2\rho'}{\partial t^2}-\Gamma'\Delta\frac{\partial\rho'}{\partial t}-v^2\Delta\rho'=\Delta p_{\mathrm{st}}\ . \tag{1}$$

Here Δ is the Laplacian, v is the adiabatic velocity of sound, Γ' is the attenuation constant of sound from viscosity, and p_{st} is the electrostrictive pressure

$$p_{\mathrm{st}}=-\gamma_e\varepsilon_0\frac{\mathbf{E}^2}{2}\ . \tag{2}$$

γ_e denotes the electrostrictive constant, which for dilute gases equals the linear susceptibility κ. In the derivation of Eq. (1) terms nonlinear in ρ' have been neglected. For optical frequencies, $\mathbf{E}^2$ in (2) is replaced by the average over an optical period. For an experimental setup with two beams $\mathbf{E}_1$ and $\mathbf{E}_2$ from one laser, intersecting at the angle θ and approximated by plane waves, the field $\mathbf{E}$ is given by

$$\mathbf{E}(\mathbf{r},t)=\mathbf{E}_1(\mathbf{r},t)+\mathbf{E}_2(\mathbf{r},t) \tag{3}$$

with

$$\mathbf{E}_1(\mathbf{r},t)=\mathbf{e}_1E_1u(t)A(t)e^{i(\mathbf{k}_1\cdot\mathbf{r}-\omega_1t)}+\text{c.c.}\ ,$$
$$\mathbf{E}_2(\mathbf{r},t)=\mathbf{e}_2E_2u(t-\tau_d)A(t)e^{i(\mathbf{k}_2\cdot\mathbf{r}-\omega_1t)}+\text{c.c.} \quad (4)$$

The amplitude $A(t)$ is assumed to be Gaussian,

$$A(t)=\left[\frac{2}{\tau}\right]^{1/2}\left[\frac{\ln 2}{\pi}\right]^{1/4}e^{-2\ln 2[(t-\bar{t})/\tau]^2}\ ,$$

with the pulse width τ [full width at half maximum (FWHM)] and the normalization

$$\int_{-\infty}^{\infty}A^2(t)dt=1\ .$$

$\mathbf{e}_i$ represents the polarization vectors, E_i complex amplitudes, and $u(t)$ a complex stochastic amplitude with $\langle|u(t)|^2\rangle=1$. $\mathbf{k}_i$ are the wave vectors with $|\mathbf{k}_i|=k$, $\bar{t}$ is the time indicating the pulse center, and τ_d is a time delay between $\mathbf{E}_1$ and $\mathbf{E}_2$, assumed to be small compared to τ. From Eqs. (3) and (4) the spatially dependent part of $\mathbf{E}^2(\mathbf{r},t)$ for parallel polarization, averaged over an optical period, is

$$\bar{\mathbf{E}}^2=2E_1E_2^*u(t)u^*(t-\tau_d)A^2(t)e^{iqx}+\text{c.c.} \quad (5)$$

with

$$\mathbf{q}=\mathbf{k}_1-\mathbf{k}_2\ ,\quad q=|\mathbf{q}|=2k\sin\left[\frac{\theta}{2}\right]\ . \quad (6)$$

The x axis is chosen to be parallel to $\mathbf{q}$. Expression (5) inserted into (2) leads to the following form of the wave equation (1):

$$\frac{\partial^2\rho'}{\partial t^2}-\Gamma'\Delta\frac{\partial\rho'}{\partial t}-v^2\Delta\rho'=\varepsilon_0\gamma_eq^2E_1E_2^*u(t)u^*(t-\tau_d)\times A^2(t)e^{iqx}+\text{c.c.} \quad (7)$$

A solution of (7) of the form

$$\rho'(t,x)=e^{iqx}K(t)+\text{c.c.}\ , \quad (8)$$

representing a standing wave, is found if $K(t)$ obeys the equation

$$\ddot{K}+q^2\Gamma'\dot{K}+q^2v^2K=\varepsilon_0\gamma_eq^2E_1E_2^*u(t)u^*(t-\tau_d)A^2(t)\ . \quad (9)$$

The solution of this equation is given in the Appendix (A4).

In case of truly stochastic variables $u(t)$ (multimode laser) the phase of the right-hand side of (9) is in general time dependent, induced by the random variables $u(t)$. $K(t)$ gets therefore a time-dependent random phase which corresponds to a random motion of the grating fringes. The phase of $K(t)$, however, is irrelevant for the grating reflectivity, which is proportional to the square $|K(t)|^2$ [see Eq. (8)]. In the following, the expectation value of $|K(t)|^2$,

$$R(t)\equiv\langle|K(t)|^2\rangle\ , \quad (10)$$

will be considered [15]. $R(t)$ is proportional to the reflectivity, averaged over many pulses. To calculate $R(t)$ the product of the u functions in the integral for $|K(t)|^2$ is replaced by the expectation value

$$\Gamma^{(4)}(t_1,t_2-\tau_d,t_1-\tau_d,t_2)\doteq\langle u(t_1)u(t_2-\tau_d)u^*(t_1-\tau_d)u^*(t_2)\rangle\ .$$

$\Gamma^{(4)}$ can be decomposed into a sum of $\Gamma^{(2)}$ expressions

$$\Gamma^{(4)}(t_1,t_2-\tau_d,t_1-\tau_d,t_2)=|\Gamma^{(2)}(\tau_d)|^2+|\Gamma^{(2)}(t_2-t_1)|^2 \quad (11)$$

if $u(t)$ exhibits Gaussian statistics, which is a good approximation for frequency-doubled Nd:YAG laser light [16]. The application of Eq. (11) leads also for non-Gaussian $U(t)$ often to an approximately correct result, namely, when $\Gamma^{(4)}$ essentially is a single product of $\Gamma^{(2)}$ functions. $R(t)$ can now be evaluated if the spectral line shape, which determines $\Gamma^{(2)}$, is known. The result for a Gaussian spectral line shape is given in (A13) and (A14). For a time t, with $t-\bar{t}>\tau''(1+\beta\tau'')$ [see (13) for definitions of β and τ''], the expression (A13) is reduced to

$$R(t)=\frac{1}{2}\left[\frac{\varepsilon_0\gamma_eq^2}{\Omega}\right]^2|E_1|^2|E_2|^2\times e^{-2\beta(t-t'')}\{P(t)+Q(t)\}\ , \quad (12)$$

$$P(t)=e^{-\pi(\tau_d/\tau_c)^2-(\Omega\tau'')^2}\{1-\cos[2\Omega(t-t')]\}\ ,$$

$$Q(t)=\left[\frac{2\ln 2}{\pi}\right]^{1/2}\frac{\tau_c}{\tau}\times\{1-e^{-(\Omega\tau'')^2}\cos[2\Omega(t-t')]\}\ ,$$

where

$$\Omega=qv\left[1-\left[\frac{q\Gamma'}{2v}\right]^2\right]^{1/2}\ ,$$
$$\beta=\tfrac{1}{2}q^2\Gamma'\ ,$$
$$\tau''=\frac{\tau}{(8\ln 2)^{1/2}}\ ,$$
$$t'=\bar{t}+\beta\tau''^2\ , \quad (13)$$
$$t''=(\bar{t}+t')/2\ ,$$
$$\tau_c=\int_{-\infty}^{\infty}|\Gamma^{(2)}(t')|^2dt'\ .$$

In the derivation of Eq. (12), it has been assumed that $|q\Gamma'/2v|<1$ and $\tau_c\ll\beta^{-1},\Omega^{-1},\tau$. The grating oscillates at an angular frequency 2Ω and decays with the constant $2\beta=q^2\Gamma'$. The ratio $Q(t)/R(t)$ gives the reduction of the grating reflectivity using temporally incoherent ($|\tau_d|\gg\tau_c$) instead of temporally coherent ($\tau_d=0$) excitation beams. In the case of $T_p\gg\tau$, where $T_p=\pi/\Omega$ is the grating period, the reduction factor is approximately the ratio of pulse duration to coherence time τ/τ_c. The reduction factor is smaller if $T_p\lesssim\tau$.

The amplitudes E_i, which appear in Eq. (12), are related to the pulse energies $W_{i,\text{pulse}}$:

$$|E_i|^2=\frac{W_{i,\text{pulse}}}{2S}\left[\frac{\mu_0}{\varepsilon_0}\right]^{1/2}, \tag{14}$$

where S is the beam cross section. The term with $P(t)$ in $R(t)$ is, up to the factor $F\equiv\exp[-(\Omega\tau'')^2]$, proportional to the pulse energies. The factor F expresses the superposition of the waves generated in any small time interval during the pulse duration. For $\tau\ll T_p$, essentially constructive superposition takes place, which is represented by $F\approx 1$. For frequencies $\Omega\gtrsim 1/\tau''$, the term $P(t)$ depends, due to F, very sensitively on Ω. This derives from the assumption of an exact Gaussian pulse envelope and is to that extent not verified by our experiments (Sec. V). [For $\Omega\gtrsim 1/\tau''$, already a small deviation from the assumed Gaussian pulse envelope $A^2(t)$ will result in a strong change of the calculated $R(t)$.] In $Q(t)$ the factor F is from the statistical average of the oscillations from single pulses.

In the derivation of Eq. (1), we assumed linearity in ρ'. The maximum value of ρ' with respect to position x [see Eq. (8)] is $\rho'_{\max}=2|K(t)|$. For argon at 5 bar, pulse energies $W_{1,\text{pulse}}=73$ mJ and $W_{2,\text{pulse}}=37$ mJ, beam diameter equal to 6 mm, and $\theta=2.9°$, which are experimental conditions used later, $\rho'_{\max}$ reaches a value of 3.0×10^{-5} Kg/m^3. This corresponds to a pressure disturbance of 3.1×10^{-5} bar, which is small enough to justify the assumption.

The dependence of the signal intensity on the gas pressure due to γ_e has been measured in air at room temperature. A quadratic relationship was found over the pressure range of 80 mbar to 5 bar (slope of the double logarithmic plot 2.089 ± 0.005). The dependence of the signal intensity I_s upon the laser intensity I_{laser} was checked in a setup with all three beams originating from the same laser. In the range of 15–90 MW/cm^2, $I_s\propto I_{\text{laser}}^{3.2\pm0.1}$ was found.

IV. VELOCITY AND ATTENUATION MEASUREMENTS OF SOUND WAVES IN GASES

Electrostrictivity generated gratings can be used to measure the velocity and the attenuation of sound waves in gases. The nonresonant nature of these gratings allows us to perform the measurements at any frequency, i.e., independent of the absorption lines of the medium under investigation. In this section the method is used for measurements in argon and nitrogen. The results are compared to the theory given in the preceding section.

The signal obtained by diffracting a probe beam off a grating is proportional to the reflectively of the grating. By changing the delay between the excitation beams and the probe beam the temporal development of the grating can be studied. The measured signal is a convolution of the grating oscillation and the temporal shape of the probe pulse. Therefore, a sufficiently small angle θ between the excitation beams has to be chosen in order to obtain an angular frequency 2Ω of the grating oscillation which still can be resolved by a probe beam with a pulse duration of 8 ns. The probe beam was delayed in steps of 2 ns. For every time delay, the signal obtained during 25 pulses was averaged. To increase further the signal to noise ratio, but minimizing the influence of a possible long-term power drift of the lasers on the measured grating reflectivity, ten such time scans were averaged. Figure 2 shows the results obtained in Ar at 5 bar. The oscillations of the grating, confirming its acoustic nature, are well visible. The dots represent the difference between measured values and a fit obtained from the convolution of Eq. (A13) with a Gaussian temporal profile, assumed to properly describe the temporal shape of the probe beam. The slowly varying background of the signal intensity arises from the convolution of the broad Gaussian probe pulse with the grating reflectivity. From the fit one can extract the values for attenuation and sound velocity. The values given below, however, have been simply determined by measuring the temporal distance and the decay of the peaks.

The adiabatic sound velocity v is given in Eq. (13) by $v=\Omega/q[1+(\beta/\Omega)^2]^{1/2}$. This can be written in the form

$$v=\frac{\lambda}{4T_p\sin\left[\frac{\theta}{2}\right]}\left[1+\left[\frac{T_p}{2\pi T}\right]^2\right]^{1/2}. \tag{15}$$

Here $T_p=\pi/\Omega$ is the period of the grating reflectivity, $T=1/2\beta$ is the decay time of the grating, and $\lambda=2\pi/k$ is the wavelength of the laser. The largest error in the determination of the sound velocity results from the measurement of the angle θ. Its approximative determination, obtained by measuring the lengths in the geometry of the two crossed excitation beams, has an estimated accuracy of 0.05°. This corresponds to an accuracy of 2% in the determination of the sound velocity. Therefore, we used the more accurate value from Ref. [17] of the sound velocity of argon to calibrate θ and the wave vector q. The so obtained value for θ was $2.926°\pm0.006°$. The acoustic frequency $\nu=\Omega/2\pi$ is 30.8 MHz.

The decay time T of the grating was determined by fitting the peak values with an exponential function. Only peaks appearing at a delay of the probe beam that is smaller than 0.5 μs were considered. During this time

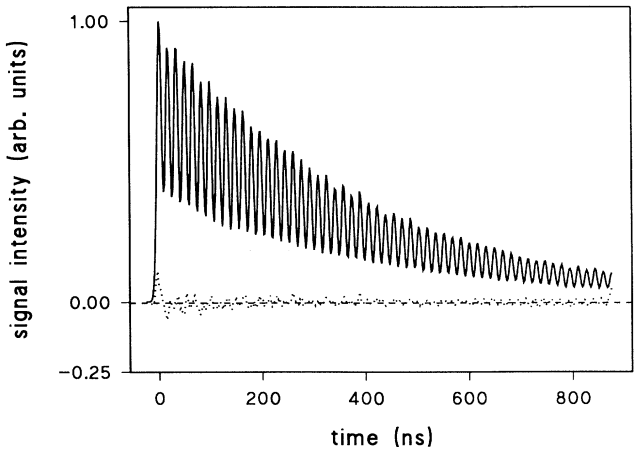

FIG. 2. Signal intensity vs time delay between excitation beams and the probe beam in Ar at 5 bar. The angle between the excitation beams is $\theta=2.926°$.

TABLE I. Attenuation constants Γ' for Ar and N_2 at 5 bar, 24 °C, and a frequency of 30.8 MHz. Γ'_m are the values measured in this work, including the statistical error. Γ'_{cl} are the values calculated from Eq. (16) and Ref. [17].

	Ar	N_2
Γ'_m (10^{-6} $m^2 s^{-1}$)	6.71±0.10	8.24±0.12
Γ'_{cl} (10^{-6} $m^2 s^{-1}$)	6.50	5.92

the sound wave propagates about 0.15 mm. The systematic error due to the propagation of the sound waves out of the overlap volume is then estimated to be less than 2%. The fit results in a decay time $T=410\pm6$ ns. Usually the values for sound attenuation are given in the quantity Γ', which is related to T by $\Gamma'=1/q^2T$. For pure monoatomic gases Γ' can be compared to the classical Kirchhoff-Stokes attenuation Γ'_{cl}, which takes into account the effect of the shear viscosity μ_s and the thermal conductivity κ:

$$\Gamma'_{cl}=\frac{\mu_s}{\rho}\left[\frac{4}{3}+\frac{\kappa}{c_p\mu_s}(\gamma-1)\right] . \tag{16}$$

Here ρ is the gas density, c_p and c_v are the specific heat capacities at constant pressure and constant volume, respectively, and $\gamma=c_p/c_v$. In Table I the values of Γ'_{cl} obtained from inserting in (16) the data of Ref. [17] are listed together with our values for the attenuation of sound determined from the experiment.

Measurements in nitrogen at 5 bar have been performed under the same experimental conditions. With the angle θ determined as described above, the velocity of sound differs by 0.3% from the value of Ref. [14], which is within the accuracy of the measurements. The obtained decay time is $T=333\pm5$ ns. In addition to thermal conductivity and shear viscosity, further dissipation mechanisms have to be taken into account in order to describe the sound attenuation in a polyatomic gas such as nitrogen (see, e.g, [18,19]). Employing Eq. (16), the calculated attenuation in nitrogen is a fraction 0.72 of the measured value Γ'_m (Table I), which is in agreement with the measurement of Greenspan [18].

V. COHERENCE EFFECTS

The calculation in Sec. III shows that the grating reflectivity and therefore the signal intensity is proportional to a sum of two terms $P(t)$ and $Q(t)$ [see Eq. (12)]. In essence they reflect the dependence of the signal intensity upon the coherence time of the laser used in this experiment. By measuring the grating reflectivity as a function of the time delay between the excitation beams it should be possible to get some evidence for the correctness of the assumption of a Gaussian frequency spectrum of the laser which has been applied in the derivation of Eq. (12). The diffracted light intensity (see Fig. 3) has been fitted by the sum of a Gaussian and a constant (solid line). A fit by the sum of a symmetric exponential function and a constant (dashed line), which would be expected in case of a Lorentzian frequency spectrum [15], has also been tried, but gives less agreement. Therefore, the

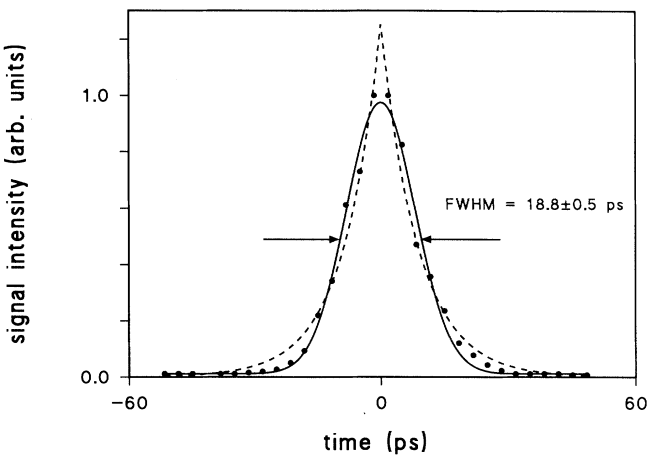

FIG. 3. Signal intensity vs time delay between the excitation beams measured in ambient air (●). The delay between the first excitation beam and the probe beam is zero. The relative error of the measured signal intensity is about 10%. The solid line is the fit by the sum of a Gaussian and a constant. The dashed line is the fit by the sum of a symmetric exponential function and a constant.

assumption of a Gaussian frequency spectrum seems to be justified. The measured FWHM of 18.8±0.5 ps, resulting from the Gaussian fit, corresponds to a coherence time τ_c of 20.1±0.5 ps, which translates into a coherence length of 6 mm and a bandwidth of 1.1 cm^{-1} of the laser. For a frequency-doubled Nd:YAG laser with a pulse length of some 10 ps Eichler, Klein, and Langhans [20] found that a Lorentzian is a more appropriate description of its frequency spectrum. However, in our measurements there is no strong evidence for a non-Gaussian contribution to the frequency spectrum, which possibly would lead, especially in the wings of Fig. 3, to a slower reduction of the grating reflectivity with increasing time delay between the two excitation beams than predicted by the Gaussian. The ratio of term $P(t)$ at $\tau_d=32$ and 0 ps was measured to be smaller than 0.02. Therefore, for a time delay between the two excitation beams, largely exceeding the coherence time, it is a reasonable assumption that the grating reflectivity is entirely due to $Q(t)$. Figure 4 shows the signal intensity versus time delay between the probe beam and the excitation beam obtained in Ar at about 5 bar, $\tau_d=65$ ps, and at a crossing angle $\theta=2.81°$. Measurements of the signal intensity were averaged as described in Sec. IV with five scans instead of ten. Even for a slightly modified correlation function one can expect that, under this condition, the contribution of $P(t)$ to the grating reflectivity is negligible. Considering the interval 95–101 ns of the time delay between excitation and probe beam, the signal intensity at $\tau_d=65$ ps was found to be smaller by a factor $(3.0\pm0.2)\times10^2$ compared to the signal intensity at $\tau_d=0$. This matches fairly well the value 4.0×10^2 calculated from Eq. (12). Another measurement of the grating reflectivity has been performed at $\tau_d=65$ and at an angle $\theta=8.3°$ corresponding to an acoustic frequency $\nu=87$ MHz. Figure 5 shows the result obtained in Ar at about 5 bar. The data were

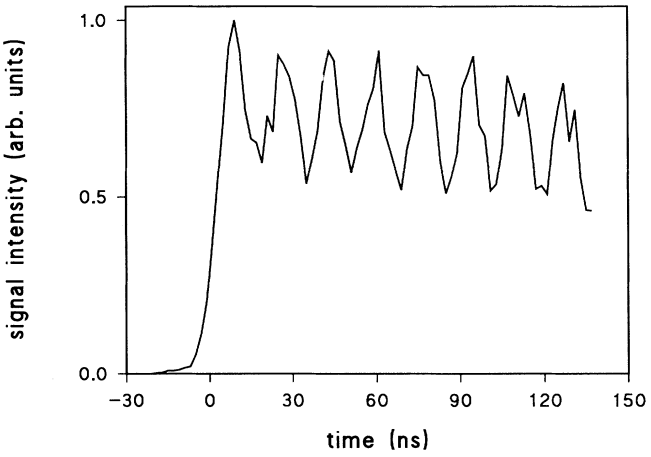

FIG. 4. Signal intensity vs time delay between the excitation beams and the probe beam measured in 5 bar Ar. The delay between the excitation beams is $\tau_d = 65$ ps and the crossing angle is $\theta = 2.81°$.

averaged as described above. For this angle, T_p is smaller than the pulse duration τ. The oscillation of the grating reflectivity is averaged out by the shape of the probe pulse. At an arbitrarily selected time delay of 17 ns between excitation and the probe beam, the signal intensity was found to be smaller by about a factor 120 ± 20 compared to the signal intensity at $\tau_d = 0$. For these experimental conditions Eq. (12) predicts a smaller factor [cf. comment on Eq. (14)].

VI. CONCLUSION

Two beams of a multimode laser with nanosecond pulses intersecting at an angle θ were used to form a nonresonant laser-induced grating in the gas phase. Its reflectivity has been investigated by scattering a probe beam from a second pulsed laser off the grating. The temporal coherence function of the excitation laser has been measured by changing the time delay between the excitation beams. The grating reflectivity is fitted with a Gaussian function rather than with a symmetric exponential function, indicating a Gaussian frequency spectrum of the laser. The wings of the coherence function show an approximately constant contribution.

The time dependence of the grating was investigated by delaying stepwise the probe beam with respect to the excitation beams. The outcome shows the damped oscillation of a decaying standing acoustic wave. Also for temporally incoherent excitation beams the formation of a nonresonant acoustic grating has been shown. This corresponds to the contribution in the coherence function which is independent of the time delay. The reflectivity of the grating generated by temporally incoherent beams is reduced for small angles θ, corresponding to large oscillation periods, by about the ratio of coherence time to pulse duration compared to the reflectivity for coherent excitation beams. The experimental results are interpreted within a calculation of electrostrictive gratings, excited by laser beams having a Gaussian temporal line shape, Gaussian statistics of the intensity, and Gaussian frequency spectrum. The fourth-order coherence function of the laser field is thereby evaluated. The calculated ratio of the grating reflectivity of coherent to incoherent excitation beams is in good agreement with the experimental value.

Electrostrictive gratings allow the measurement of sound velocity and attenuation at nonresonant frequencies of the medium. Measurements of these quantities have been performed for Ar and N_2. The application of the technique for practical purposes is under investigation and will be published elsewhere.

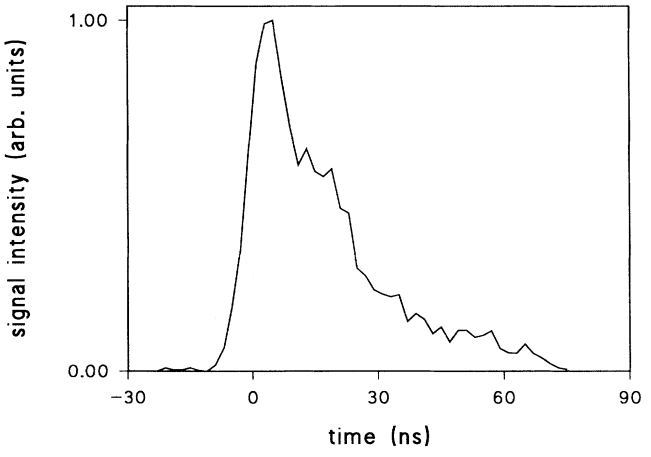

FIG. 5. Signal intensity vs time delay between the excitation beams and the probe beam measured in 5 bar Ar. The delay between the excitation beams is $\tau_d = 65$ ps and the crossing angle is $\theta = 8.3°$.

ACKNOWLEDGMENTS

The authors would like to thank B. Käppeli for his technical support. Helpful discussions with P. Talkner are gratefully acknowledged. This work was supported by the Swiss Federal Office of Energy (BEW).

APPENDIX

The solution of the equation

$$\ddot{G} + q^2\Gamma'\dot{G} + q^2v^2G = \delta(t) \tag{A1}$$

vanishing for $t < 0$ and, assuming $|q\Gamma'/2v| < 1$, is

$$G(t) = \frac{1}{\Omega}\sin\Omega t e^{-\beta t}\Theta(t) , \tag{A2}$$

where

$$\Omega = qv\left[1 - \left[\frac{q\Gamma'}{2v}\right]^2\right]^{1/2} ,$$

$$\beta = \tfrac{1}{2}q^2\Gamma' , \tag{A3}$$

$$\Theta(t) = \begin{cases} 1 , & t > 0 \\ 0 , & t < 0 . \end{cases}$$

Therefore, the solution of Eq. (9) is the convolution

$$K(t)=\varepsilon_0\gamma_e q^2 E_1 E_2^* \frac{2}{\Omega\tau}\left[\frac{\ln 2}{\pi}\right]^{1/2} \times\int_{-\infty}^{t} u(t_1)u^*(t_1-\tau_d)\exp\left[-\left[\frac{t_1-\bar{t}}{\tau'}\right]^2\right] \times\sin\Omega(t-t_1)\exp[-\beta(t-t_1)]dt_1 , \quad \text{(A4)}$$

where

$$\tau'=\frac{\tau}{2(\ln 2)^{1/2}} . \quad \text{(A5)}$$

$R(t)$, defined in (10), is then

$$R(t)=4(\varepsilon_0\gamma_e q^2)^2|E_1|^2|E_2|^2\frac{1}{(\Omega\tau)^2}\frac{\ln 2}{\pi}S(t) , \quad \text{(A6)}$$

where

$$S(t)=\int_{-\infty}^{t}\int_{-\infty}^{t}\langle u(t_1)u(t_2-\tau_d)u^*(t_1-\tau_d)u^*(t_2)\rangle \times e^{-x_1^2}e^{-x_2^2}\sin\Omega(t-t_1)\sin\Omega(t-t_2) \times e^{-\beta(t-t_1)}e^{-\beta(t-t_2)}dt_1dt_2 \quad \text{(A7)}$$

with

$$x_i=\frac{t_i-\bar{t}}{\tau'} .$$

The fourth-order correlation function

$$\Gamma^{(4)}(t_1,t_2-\tau_d,t_1-\tau_d,t_2) =\langle u(t_1)u(t_2-\tau_d)u^*(t_1-\tau_d)u^*(t_2)\rangle \quad \text{(A8)}$$

can be decomposed for a Gaussian $u(t)$ into functions $\Gamma^{(2)}$ [21]. For a Gaussian spectral line shape it takes the form

$$\Gamma^{(4)}(t_1,t_2-\tau_d,t_1-\tau_d,t_2) =e^{-\pi(\tau_d/\tau_c)^2}+e^{-\pi[(t_1-t_2)/\tau_c]^2} . \quad \text{(A9)}$$

τ_c is the coherence time.

Equations (A8) and (A9) inserted into (A7) lead to

$$S(t)=e^{-\pi(\tau_d/\tau_c)^2}I_1^2+\tau_c I_2 , \quad \text{(A10)}$$

where

$$I_1=\int_{-\infty}^{t} e^{-x_1^2}e^{-\beta(t-t_1)}\sin[\Omega(t-t_1)]dt_1 , \quad \text{(A11)}$$

$$I_2=\int_{-\infty}^{t} e^{-2x_2^2}e^{-2\beta(t-t_1)}\sin^2[\Omega(t-t_1)]dt_1 . \quad \text{(A12)}$$

It has been used here that τ_c is small compared to the other time scales. With the help of formulas (2.3.15.4) and (2.5.36.8) of Ref. [22], the integrals I_1 and I_2 [(A11) and (A12)] can be expressed by known functions

$$S(t)=\pi\tau''^2 e^{-2\beta(t-t'')}\left\{e^{-\pi(\tau_d/\tau_c)^2}e^{-(\Omega\tau'')^2}C(t)+\left[\frac{2\ln 2}{\pi}\right]^{1/2}\frac{\tau_c}{\tau}\left[1-\frac{1}{2}\operatorname{erfc}\Theta'-e^{-(\Omega\tau'')^2}D(t)\right]\right\} , \quad \text{(A13)}$$

where

$$\operatorname{erfc}(z)=1-\operatorname{erf}(z) , \quad \operatorname{erf}(z)=\frac{2}{\pi^{1/2}}\int_0^z\exp(-t^2)dt ,$$

$$C(t)=[1-\tfrac{1}{2}\operatorname{Re}\operatorname{erfc}(\Theta''')]^2\{1-\cos[2\Omega(t-t')]\} +[1-\tfrac{1}{2}\operatorname{Re}\operatorname{erfc}(\Theta''')]\operatorname{Im}\operatorname{erfc}(\Theta''')\sin[2\Omega(t-t')] +\tfrac{1}{4}[\operatorname{Im}\operatorname{erfc}(\Theta''')]^2\{1+\cos[2\Omega(t-t')]\} , \quad \text{(A14)}$$

$$D(t)=[1-\tfrac{1}{2}\operatorname{Re}\operatorname{erfc}(\Theta'')]\cos[2\Omega(t-t')]+\tfrac{1}{2}\operatorname{Im}\operatorname{erfc}(\Theta'')\sin[2\Omega(t-t')] ,$$

$$\Theta'=\frac{t-\bar{t}}{\tau''}-\beta\tau'' , \quad \tau''=\frac{\tau}{(8\ln 2)^{1/2}} ,$$

$$\Theta''=\Theta'+i\Omega\tau'' , \quad \Theta'''=2^{-1/2}\Theta'' , \quad t'=\bar{t}+\beta\tau''^2 , \quad \tau''=(\bar{t}+t')/2 .$$

[1] H. J. Eichler, P. Günter, and D. W. Pohl, *Laser-Induced Dynamic Gratings* (Springer, Berlin, 1986).

[2] T. Y. Chang, Opt. Eng. **20**, 220 (1981).

[3] Z. Yu, X. Mi, Q. Jiang, P. Ye, and P. Fu, Opt. Lett. **13**, 117 (1988). P. Fu, Z. Yu, X. Mi, Q. Jiang, and Z. Zhang, Phys. Rev. A **46**, 1530 (1992).

[4] M. A. Buntine, D. W. Chandler, and C. C. Hayden, J. Chem. Phys. **97**, 707 (1992).

[5] M. D. Wheeler, I. R. Lambert, and M. N. R. Ashfold, Chem. Phys. Lett. **211**, 381 (1993).

[6] J. A. Gray, J. E. M. Goldsmith, and R. Trebino, Opt. Lett. **18**, 444 (1993).

[7] E. F. McCormack, S. T. Pratt, P. M. Dehmer, and J. L. Dehmer, Chem. Phys. Lett. **211**, 147 (1993).

[8] G. Hall and B. J. Whitaker, J. Chem. Soc. Faraday Trans. **90**, 1 (1994).

[9] K. A. Nelson, D. R. Lutz, M. D. Fayer, and L. Madison, Phys. Rev. B **24**, 3261 (1981); K. Nelson, R. J. D. Miller,

D. R. Lutz, and M. D. Fayer, J. Appl. Phys. **53**, 1144 (1982).

[10] Y. Yan and K. A. Nelson, J. Chem. Phys. **87**, 6240 (1987); **87**, 6257 (1987); Y. Yan, L. Cheng, and K. A. Nelson, in *Advances in Non-linear Spectroscopy,* edited by R. S. H. Clark and R. E. Hester (Wiley, New York, 1988).

[11] D. E. Govoni, J. A. Booze, A. Sinha, and F. F. Crim, Chem. Phys. Lett. **216**, 525 (1993).

[12] B. Hemmerling and A. Stampanoni-Panariello, Appl. Phys. B **57**, 281 (1993).

[13] A. E. Siegman, J. Opt. Soc. Am. **67**, 545 (1977).

[14] R. W. Boyd, *Nonlinear Optics* (Academic, New York, 1992), Chap. 8.6. For a process with heat transfer a coupled system of equations for $\rho'(t,\mathbf{r})$ and the temperature $T(t,\mathbf{r})$ has to be solved.

[15] R. Trebino, E. K. Gustafson, and A. E. Siegman, J. Opt. Soc. Am. B **3**, 1295 (1986).

[16] W. Hubschmid, R. Bombach, and T. Gerber, Appl. Opt. **33**, 5509 (1994). Note that the measurements in this article were performed with a frequency-doubled Nd:YAG laser working with an étalon.

[17] *Encyclopédie des Gaz* (Elsevier, Amsterdam, 1976); *American Institute of Physics Handbook* (McGraw-Hill, New York, 1963). All data except the specific heats have been taken from the first reference. For γ the value at 15 °C and 1 atm has been taken.

[18] M. Greenspan, J. Acoust. Soc. Am. **31**, 155 (1959). Γ'_{cl} accounts for a fraction 0.74 of the measured value Γ' of this reference.

[19] J. J. Markham, R. T. Beyer, and R. B. Lindsay, Rev. Mod. Phys. **23**, 353 (1951); H. O. Kneser, in *Acoustics I,* edited by S. Flügge, Encyclopedia of Physics Vol. XI/1 (Springer, Berlin, 1961).

[20] H. J. Eichler, U. Klein, and D. Langhans, Appl. Phys. **21**, 215 (1980).

[21] J. W. Goodman, *Statistical Optics* (Wiley, New York, 1985).

[22] A. P. Prudnikov, Yu. A. Brychkov, and O. I. Marichev, *Integrals and Series* (Gordon and Breach, New York, 1986), Vol. 1.